

Nonequilibrium Phenomenology of Identified Particle Spectra in Heavy-Ion Collisions at LHC Energies

Oleksandr Vitiuk,¹ David Blaschke,^{1,2,3} Benjamin Dönigus,⁴ and Gerd Röpke⁵

¹*Institute of Theoretical Physics, University of Wrocław, Plac Maza Borna, 50-204 Wrocław, Poland*

²*Center for Advanced Systems Understanding (CASUS), Untermarkt 20, D-02826 Görlitz, Germany*

³*Helmholtz-Zentrum Dresden-Rossendorf (HZDR),*

Bautzener Landstrasse 400, D-01328 Dresden, Germany

⁴*Institut für Kernphysik, Goethe Universität Frankfurt am Main,*

Max-von-Laue-Str. 1, D-60438 Frankfurt am Main, Germany

⁵*Institute of Physics, University of Rostock, Albert-Einstein Str. 23-24, D-18059 Rostock, Germany*

(Dated: September 16, 2024)

A nonequilibrium state does not relax to thermodynamic equilibrium but to a state which takes into account long-living fluctuations as quasi-conserved quantities. This state is described by the relevant statistical operator within the Zubarev method to derive the nonequilibrium statistical operator. We apply this approach to the spectra of particles produced in ultrarelativistic heavy ion collisions at the LHC experiments at CERN. We show that controversial explanations of the low-momentum part of the spectrum given by an extended hydrodynamic-like Blast-Wave approach [with mesonic chemical potentials] and the reaction-kinetic description of the hadron resonance gas can be considered as special approximation of a more general nonequilibrium approach which takes mesonic chemical potentials into account to describe quasi-conserved particle numbers, but takes also continuum correlations, in particular resonances, into account using the Beth-Uhlenbeck [or Dashen-Ma-Bernstein] virial expansion. We present results for the spectra of pions, kaons, and protons and explain why different approaches can explain the data obtained from the ALICE experiments.

Since the early days of ultrarelativistic heavy-ion collisions at CERN-SPS the yields and spectra of identified particles have been the key observables to deduce the thermodynamic properties of the state of matter that has been created in these collisions [1]. In order to understand the emergence of hadronic yields from the nonequilibrium process of the hadronization of the quark-gluon plasma, a flavor-kinetic model has been developed [2, 3]. However, soon after this development it has been demonstrated that the particle yields could nicely be described within a simple chemical freeze-out model from the statistical equilibrium state of hadrons with just two parameters, the freeze-out temperature and freeze-out chemical potential. As a caveat of such a description, the spectra of pions (and kaons) at low transverse momenta could not be described well with equilibrium distribution functions. A nonequilibrium distribution function with a finite pion (and kaon) chemical potential could well describe the observed enhancement in the low transverse momentum part of the spectrum as a precursor of Bose-Einstein condensation [4]. Alternatively, the feed-down from resonance decays and the effect of radial flow has been considered [5] and gave a satisfactory description of the spectra which afterwards has been adopted as a standard tool in the theoretical description of particle spectra.

With the advent of high-precision and high-statistics data of (identified) particle production from the ALICE experiment at CERN-LHC [6, 7], the problem of a precise description of the low-momentum pion spectra came up again [8]. As a possible explanation, besides the description by anisotropic viscous hydrodynamics [9] or critical enhancement of soft pions by fluctuations at the chiral

transition [10], also the nonequilibrium statistical hadronisation model with quark fugacity factors [11] has been considered.

In this work, we present a systematic nonequilibrium approach to the pion production within the Zubarev approach and apply it to a description of the recent experimental data. To this end we will develop and use a generalized blast-wave model that takes into account the full quantum degeneracy of pion and kaon distribution functions (with a nonequilibrium chemical potential) and include also the effects of radial flow, resonance decays and final state interactions.

In contrast to low-energy scattering experiments which are described by the Schrödinger equation including a potential, the HIC demand another approach because of the large number of states which are contributing at high energy collision experiments. Therefore, a quantum statistical description is needed, based on the time-dependent statistical operator $\rho(t)$. Whereas the statistical approach is generally accepted in HIC physics, a systematic nonequilibrium approach is far from being rigorously solved. In a simple approximation, the single-particle distribution function is considered, and the Boltzmann-Uhling-Uhlenbeck equation is solved, which contains the scattering cross section and respects the Pauli principle. However, the inclusion of correlations is notoriously difficult and often taken into account in a semiempirical way, for instance the coalescence model [12]. We present the method of the nonequilibrium statistical operator (NSO) [13] which is a fundamental approach to describe nonequilibrium processes.

To determine the statistical operator $\rho(t)$ for a nonequilibrium process, we have to solve the Liouville-

von Neumann equation $\frac{\partial}{\partial t}\rho(t) = \frac{i}{\hbar}[H, \rho(t)]$ with given initial conditions. These initial conditions are represented by the average values of a set of relevant observables $\{B_i\}$ in the past $t' \leq t$ which characterize the state of the system. This information is used to construct the relevant statistical operator $\rho_{\text{rel}}(t')$ as the maximum of information entropy $S_{\text{inf}}(t') = -\langle \rho_{\text{rel}}(t') \rangle_{\text{rel}}$ under given constraints, the self-consistency conditions

$$\langle B_i \rangle^{t'} = \text{Tr} \{ \rho_{\text{rel}}(t') B_i \}. \quad (1)$$

As well known from equilibrium statistics, these self-consistency conditions are taken into account via Lagrange parameters $\lambda_i(t')$, and we obtain the generalized Gibbs distribution. The Lagrange parameters $\lambda_i(t')$ must be eliminated using the self-consistency conditions (1) which are the nonequilibrium generalizations of the equations of state. The solution of the Liouville-von Neumann equation at given boundary conditions (1) is

$$\rho(t) = \lim_{\epsilon \rightarrow 0} \epsilon \int_{-\infty}^t dt' e^{-\epsilon(t-t')} e^{-\frac{i}{\hbar}H(t-t')} \rho_{\text{rel}}(t') e^{\frac{i}{\hbar}H(t-t')}. \quad (2)$$

A particular problem of the method of NSO is the selection of the set of relevant observables $\{B_i\}$. We have to consider long-living fluctuations because they need a long time to be built up dynamically and demand higher orders of perturbation theory. A minimum set of relevant observables are the conserved observables energy H as well as the particle numbers N_i . The solution is the generalized Gibbs distribution $\rho_{\text{rel}} \propto \exp[-(H - \lambda_i N_i)/\lambda_T]$. Note that these Lagrange multipliers $\lambda_{i,T}$, which are in general time dependent (and for the hydrodynamical approach also depending on position), are not identical with the equilibrium parameters T and μ_i but may be considered as nonequilibrium generalizations of temperature

and chemical potentials.

The freeze-out approach often used to describe particle production in HIC uses local thermodynamic equilibrium with the corresponding densities of conserved quantities as set of relevant operators. If the relaxation of fluctuations is fast, i.e. the relaxation time τ_r of any fluctuation in the state described by $\rho_{\text{rel}}(t)$ is short, the limit $\epsilon \rightarrow 0$ in Eq. (2) can be replaced by $\epsilon \leq 1/\tau_r$, the memory of the system is short (Markov limit). Then, $\rho(t)$ can be replaced by $\rho_{\text{rel}}(t)$. The time evolution of the system is described by the relevant distribution which freezes out if the processes which change the distribution slow down. After freeze-out, an afterburner describes the decay of excited states feeding the stable states observed as final distribution. This evolution to the final distribution is given by reaction kinetics.

The method of NSO allows the possibility to extend the set of relevant observables $\{B_i\}$ what improves quick convergence at $\epsilon \rightarrow 0$. To derive kinetic equations, the occupation numbers of the quasiparticle states should be taken as the set of relevant observables. The corresponding Lagrange parameters which appear in the generalized Gibbs distribution are related to the single particle distribution function, and the Boltzmann equation is obtained. However, energy conservation is violated, and the equilibrium solution is the ideal quantum gas, without any correlations. The inclusion of few-particle correlations in the set of relevant observables would improve the kinetic theory and, in addition, gives the possibility to describe the formation of few-nucleon bound states.

To describe particle production at LHC energies, we employ the Blast-Wave model in its standard form, assuming freeze-out happens on the boost-invariant and cylindrically symmetric hypersurface at a constant value of the proper time $\tau = \sqrt{t^2 - z^2} = \text{const}$. Then the resulting particle distribution function is given as:

$$\frac{d^6 N_i}{dp_T dy d\eta dr d\phi d\psi} = \frac{g_i \tau r p_T m_T}{(2\pi\hbar)^3} \cosh(y - \eta) \left(\exp \left[\frac{m_T \cosh \rho \cosh(y - \eta) - p_T \sinh \rho \cos(\phi - \psi) - \mu_i}{T} \right] + a_i \right)^{-1}, \quad (3)$$

where r is the transverse radius, ϕ is the azimuthal angle in coordinate space, η is the space-time rapidity, p_T is the particle transverse momentum, m_T is the particle transverse mass, ψ is the azimuthal angle in momentum space, and y is the particle rapidity, T is the freeze-out temperature, g_i and μ_i are the spin degeneracy factor and chemical potential of the i -th particle species correspondingly with $a_i = +1$ for fermions and $a_i = -1$ for bosons. ρ is the velocity profile, parameterized as:

$$\rho = \tanh^{-1} \left[\beta_S \left(\frac{r}{R} \right)^n \right], \quad (4)$$

with the profile exponent n and transverse expansion velocity at the surface β_S . For resonances with finite width, we include additional mass attenuation in the form of the

Breit-Wigner distribution. The particle chemical potential is defined as $\mu_i = \mu_\pi Q_i^\pi + \mu_K Q_i^K$, where Q_i^π (Q_i^K) is one for pions (kaons) and zero for all other particles. μ_π and μ_K are corresponding pion and kaon effective chemical potentials. Since particle-antiparticle ratios in the energy range of interest are approximately unity over a broad transverse momentum range, we set baryon, strangeness, and electric charge chemical potentials to zero. This reduces the number of free parameters while maintaining a reasonable fit quality.

First, we perform a standard combined Blast-Wave fit of identified particle spectra to learn about the system properties on the kinetic freeze-out hypersurface. In this work, we use the identified particle invariant transverse

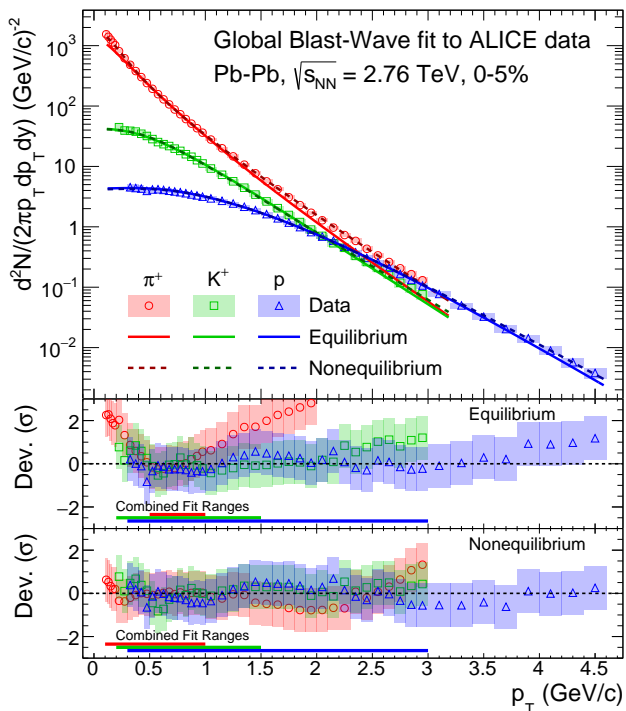


FIG. 1. Transverse-momentum spectra of π^+ , K^+ , and p (anti-particles are not shown) measured by the ALICE collaboration [6] in 0-5% central PbPb collisions at $\sqrt{s_{NN}} = 2.76$ TeV compared to the conventional Blast-Wave fit and to the fit with nonequilibrium distribution function.

momentum spectra of π^\pm , K^\pm , p , and \bar{p} measured by the ALICE collaboration in 0-5% central PbPb collisions at $\sqrt{s_{NN}} = 2.76$ TeV [6, 14].

The Blast-Wave function (3) is fitted to the data by minimizing the χ^2 over the combined fit range. Following the experimental procedure [6, 15, 16], we set the combined fit p_T ranges to 0.5 – 1.0 GeV/c for π^\pm , 0.2 – 1.5 GeV/c for K^\pm , and 0.3 – 3.0 GeV/c for (anti-)protons [6]. To examine the overall fit quality, we introduce χ^{2*} , which is the χ^2 function evaluated for all spectra over the $p_T \in [0, 2]$ GeV/c.

Since the pion number is not conserved, the chemical potential should be zero. But, comparing the pion spectra obtained from local thermodynamic equilibrium with the observed spectra, the enhancement is seen in the low-momentum part of the spectrum, see Fig. 1. Similar behaviour is seen for the kaon spectra.

To solve the puzzle of the low-momentum enhancement of the pion spectra in HIC at ultrarelativistic energies [16] we apply the method of the NSO. Two different scenarios have been proposed: i) Introduction of the pion (and kaon) chemical potential μ_π (μ_K) in the Bose distribution function [4, 17], and ii) Explicit consideration of resonances and final state interactions which feed the observed pion yields and modify the spectra after decay.

We show that both approaches are possible scenarios to describe the expanding fireball produced in HIC, but

both have only approximate validity.

Following scenario i), we introduce the non-equilibrium pion and kaon chemical potentials μ_π and μ_K into the Blast-Wave function (3). To properly infer these additional parameters, we extend the p_T fit range for pions to 0.1 – 1.0 GeV/c, while keeping the other fit ranges unchanged. The fit result is shown in Fig. 1 and fit parameters are summarized in Table I. The conventional approach with equilibrium assumption gives similar results to that obtained in the publication where data was presented [6]. Namely, the temperature is about 95 MeV, and the surface velocity is about 87% of the speed of light, whereas the nonequilibrium approach gets significantly higher temperatures, i.e. about 120 MeV at roughly the same flow velocity. The pion and kaon chemical potentials are high with $\mu_\pi = (126.2 \pm 3.8)$ MeV and $\mu_K = (402.9 \pm 22.6)$ MeV close to their masses. One can see that such an extension gives not only the correct pion (kaon) particle density but also the spectrum using just two additional parameters. Also, it is remarkable that the fit with the extended model describes the data over a broad p_T range, even outside of the fit ranges since χ^{2*} is 6.7 times better in the extended model with finite effective chemical potentials.

In the scenario ii), we have to explicitly account for resonance decays and final state interactions between hadrons. This, in fact allows us to learn about the system properties at the chemical freeze-out stage. For this purpose, we developed a Blast-Wave-based thermal particle generator coupled with the SMASH hadronic transport model [18] as an afterburner. First, for a given set of model parameters, we sample the particles' positions, momenta, and, for unstable states, masses on the freeze-out hypersurface using the previously obtained distribution function (3). We use all hadronic states from the SMASH particle list that do not contain charm and bottom quarks. Then, the particles generated from the freeze-out hypersurface are input into the SMASH model which serves as an afterburner, performing resonance decays, elastic scatterings, and other final state interactions. Also, here we challenge the assumption of the thermal equilibrium on the hadronization surface and consider two cases: with and without nonequilibrium pion chemical potential.

To infer the model parameters we use the Bayesian analysis workflow similar to one used in [19], since now the model is computationally expensive and a simple fit is not possible. The marginal posterior probability distributions of the model parameters together with the mode values and 90% credible intervals are shown in Fig. 2 for both cases. The maximum a posteriori estimates (MAP) are shown in Fig. 3 and are summarized in Table I. The Bayesian analysis using a Blast-Wave model coupled to SMASH gives a posterior temperature that is about 156 MeV, which is consistent with lattice QCD and statistical hadronization models, and a mean flow velocity of about 77% of the speed of light. These values stay stable when the chemical potential of the pion is added which

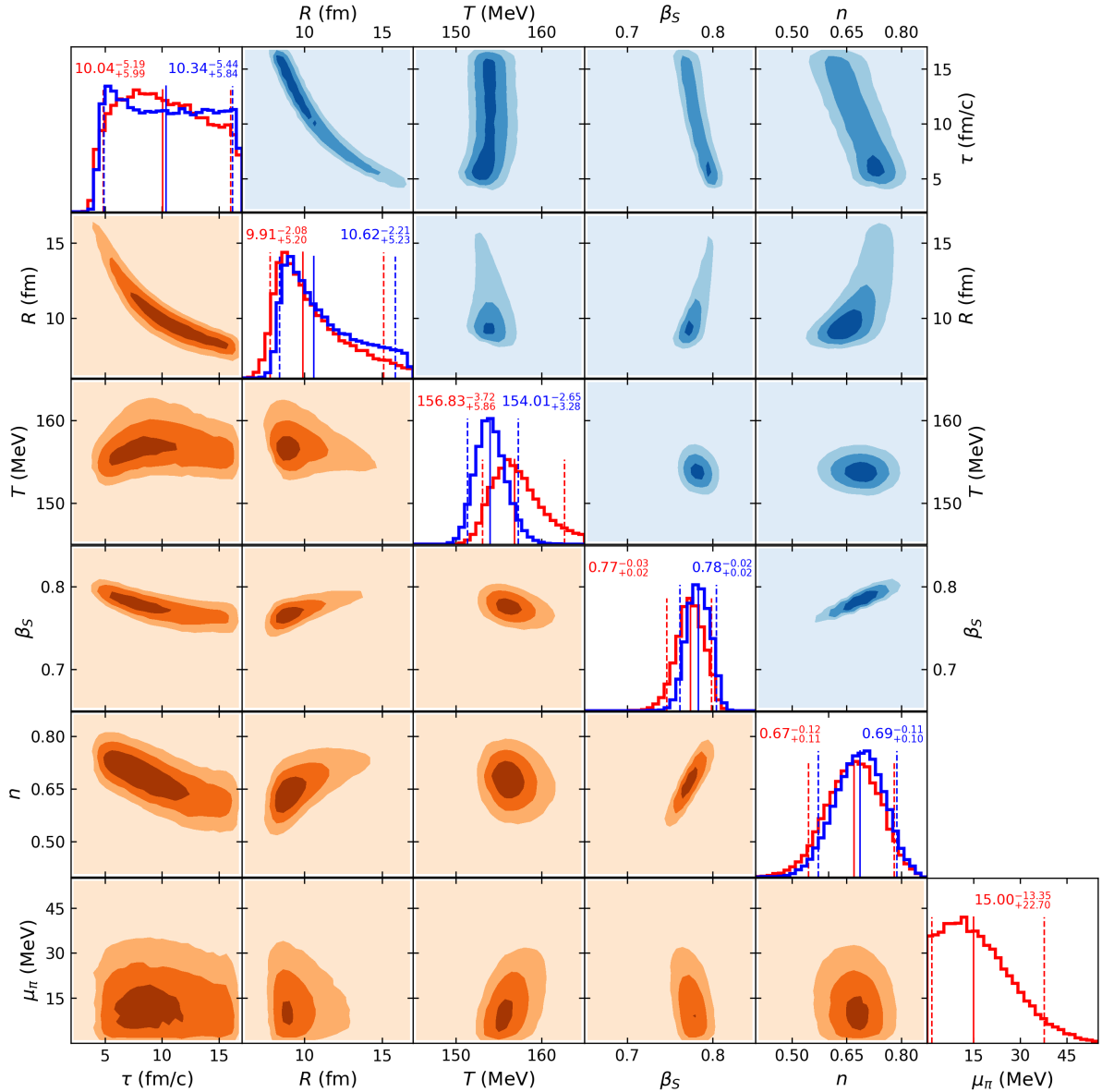


FIG. 2. Marginal (on diagonal) and joint marginal posterior probability distributions of model parameters for conventional (blue, upper triangle) and extended (orange, lower triangle) models. Solid and dashed vertical lines and numeric values indicate median values and 90% credible intervals of the parameter distributions, respectively.

is found to be $\mu_\pi \approx 9$ MeV. Also, one can see that the introduction of the nonequilibrium pion chemical potential at chemical freeze-out does not improve the description since both χ^2 and χ^{2*} stay the same. To properly compare the two assumptions, we calculated the Bayes factor. The obtained value $B_{\mu_\pi \neq 0}^{\mu_\pi = 0} = 0.434$, according to Jeffreys classification [20], means small evidence against the model with nonequilibrium chemical potential. It is a consequence of the natural penalization of the model. With no substantial improvement of the data description, the larger the number of parameters the more spread are posterior distributions.

We show that both approaches i) and ii) describe the same scenario in different approximation. The main issue is the solution of Eq. (1) which has the meaning as equation of state. It relates temperature and chemical potential to the particle number.

In simplest approximation, considering the pion system as ideal, noninteracting Bose gas, and taking the equilibrium value $\mu_\pi = 0$, we obtain the well-known result for the density of pions as a function of T . However, we have to take the interaction of pions into account. Then, the spectral function of the pion propagator becomes more complex. The evaluation of Eq. (1) with

Model	τ (fm/c)	R (fm)	T (MeV)	β_S	n	μ_π (MeV)	μ_K (MeV)	χ^2/ndof	χ^{2*}/ndof
KFO Equilibrium	-	-	97.7 ± 3.9	0.879 ± 0.005	0.709 ± 0.019	-	-	0.148	0.956
KFO Nonequilibrium	-	-	118.1 ± 3.7	0.858 ± 0.005	0.662 ± 0.023	126.2 ± 3.8	402.9 ± 22.6	0.136	0.143
CFO Equilibrium	8.88	11.54	154.02	0.786	0.699	-	-	0.1	0.1
CFO Nonequilibrium	8.08	11.5	155.98	0.783	0.697	9.52	-	0.1	0.1

TABLE I. Results of the combined blast-wave fits of identified particle spectra at kinetic freeze-out (KFO) and MAP estimate of the model parameters from the Bayesian analysis at the chemical freeze-out (CFO) for equilibrium and nonequilibrium models.

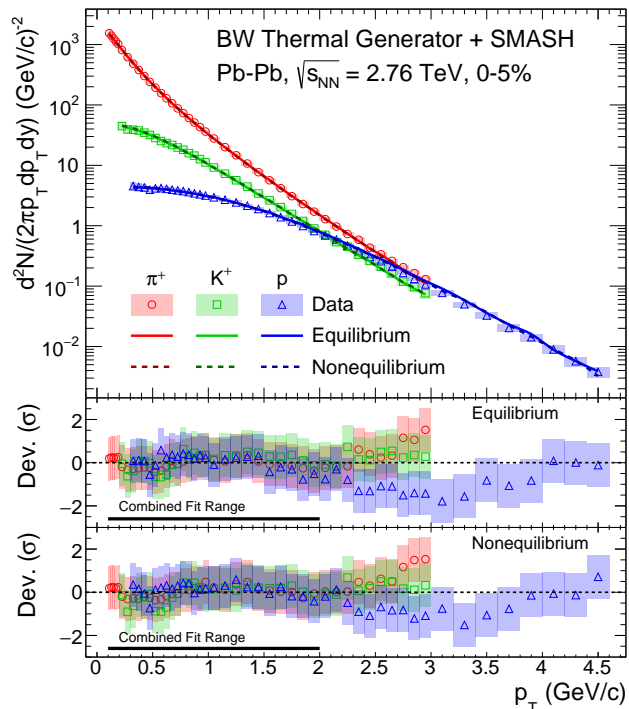


FIG. 3. Transverse momentum spectra of pions, kaons, and protons (anti-particles are not shown) compared to the maximum a posteriori estimate from the full model.

$\rho_{\text{rel}}(t)$ with Lagrange parameters T , but $\mu_\pi = 0$, leads to the Beth-Uhlenbeck result [21]

$$n_{\pi^\pm,0} = 3 \int \frac{d^3p}{(2\pi)^3} \int \frac{d\omega}{\pi T} \frac{1}{e^{\omega/T} - 1} \delta_\pi(\omega, p). \quad (5)$$

This expression of the second virial coefficient can be improved including medium effects what leads to the generalized Beth-Uhlenbeck formula. Note that all resonances are contained in the phase shifts $\delta_\pi(\omega, p)$, also with the corresponding width. Using the known scattering phase shifts, it was possible to calculate the pion yields at freeze-out $T_{\text{cf}} = 156$ MeV in good agreement with experiments [16]. In particular, the contributions from the resonances are taken into account.

The reaction-kinetic approach (SMASH) confirms this result, the microscopic treatment of reaction processes in both directions will reproduce in the dense state the equilibrium solution. For this, it is indispensable to consider

the reactions in both directions so that the detailed balance holds as prerequisite for equilibrium, and resonances should be taken into account. The scenario ii) gives a reasonable description. However, medium effects which modify the quasiparticle energies and reaction cross sections, are not contained in this approximation (e.g. the width of the ρ resonance).

The blast-wave model (scenario i)) follows the evolution until the kinetic freeze-out. The (elastic) collisions between the particles die out, and the spectrum freezes out to the final form seen in the experiment. During this stage, the number of pions remains constant, since their decay is a weak process which is sufficiently slow that the pion number $N_{\pi^\pm,0}$ becomes a quasi-conserved observable which must be included in the set of relevant observables $\{B_i\}$. Since T is changed, the condition (1) has to be used to determine the nonequilibrium chemical potential of pions. Because the temperature is low, the contribution of higher resonances in (5) is less important. (The ideal Bose gas is a simple approximation, but can be improved if resonances are considered.) We have the situation that collisions thermalize the spectrum until kinetic freeze-out, and this state is described nearly as ideal Bose gas, but with a finite chemical potential.

In conclusion, both scenarios can be considered as approximation to describe the expanding fireball. SMASH gives a microscopic description of the collision processes up to kinetic freeze-out what can be replaced by the generalized Gibbs distribution $\rho_{\text{rel}}(t)$ with the nonequilibrium μ_π to realize N_π . SMASH can be improved considering in-medium corrections, and the hydrodynamical blast-wave approach can be improved considering the Beth-Uhlenbeck formula instead of the ideal Bose gas, followed by the afterburner process.

ACKNOWLEDGMENTS

D.B. was supported by NCN under grant No. 2021/43/P/ST2/03319, O.V. received support from NCN under grant No. 2022/45/N/ST2/02391 and G.R. acknowledges a stipend from the Foundation for Polish Science within the Alexander von Humboldt programme under grant No. DPN/JJL/402-4773/2022. B.D. acknowledges support from Bundesministerium für Bildung und Forschung through ErUM-FSP T01, Förderkennzeichen 05P21RFCA1. Calculations have been carried out using resources provided by Wrocław Centre for Networking and Supercomputing, grant No. 570.

-
- [1] H. Satz, H. J. Specht, and R. Stock, eds., *QUARK MATTER. PROCEEDINGS, 6TH INTERNATIONAL CONFERENCE ON ULTRARELATIVISTIC NUCLEUS NUCLEUS COLLISIONS, NORDKIRCHEN, F.R. GERMANY, AUGUST 24-28, 1987*, Vol. 38 (1988).
- [2] H. W. Barz, B. L. Friman, J. Knoll, and H. Schulz, Flavor Kinetics in an Expanding Quark - Gluon Plasma, *Nucl. Phys. A* **484**, 661 (1988), [Erratum: *Nucl.Phys.A* 492, 663–663 (1989)].
- [3] H. W. Barz, B. L. Friman, J. Knoll, and H. Schulz, Strangeness production in ultrarelativistic heavy ion collisions: Flavor kinetics. 2., *Nucl. Phys. A* **519**, 831 (1990).
- [4] M. Kataja and P. V. Ruuskanen, Nonzero Chemical Potential and the Shape of the p_T Distribution of Hadrons in Heavy Ion Collisions, *Phys. Lett. B* **243**, 181 (1990).
- [5] E. Schnedermann, J. Sollfrank, and U. Heinz, Thermal phenomenology of hadrons from 200A GeV S+S collisions, *Phys. Rev. C* **48**, 2462 (1993).
- [6] B. Abelev and et al. (ALICE Collaboration), Centrality dependence of π , K , and p production in Pb-Pb collisions at $\sqrt{s_{NN}} = 2.76$ TeV, *Phys. Rev. C* **88**, 044910 (2013).
- [7] S. Acharya *et al.* (ALICE), Production of charged pions, kaons, and (anti-)protons in Pb-Pb and inelastic pp collisions at $\sqrt{s_{NN}} = 5.02$ TeV, *Phys. Rev. C* **101**, 044907 (2020), arXiv:1910.07678 [nucl-ex].
- [8] A. Mazeliauskas and V. Viskavicius, Temperature and fluid velocity on the freeze-out surface from π , K , and p spectra in pp , p -Pb, and Pb-Pb collisions, *Phys. Rev. C* **101**, 014910 (2020).
- [9] U. Heinz, D. Liyanage, and C. Gantenberg, Bayesian calibration of viscous anisotropic hydrodynamic (VAH) simulations of heavy-ion collisions (2023), arXiv:2311.03306 [nucl-th].
- [10] E. Grossi, A. Soloviev, D. Teaney, and F. Yan, Soft pions and transport near the chiral critical point, *Phys. Rev. D* **104**, 034025 (2021), arXiv:2101.10847 [nucl-th].
- [11] V. Begun, W. Florkowski, and M. Rybczynski, Explanation of hadron transverse-momentum spectra in heavy-ion collisions at $\sqrt{s_{NN}} = 2.76$ TeV within a chemical nonequilibrium statistical hadronization model, *Phys. Rev. C* **90**, 014906 (2014).
- [12] A. Z. Mekjian, Explosive nucleosynthesis, equilibrium thermodynamics, and relativistic heavy-ion collisions, *Phys. Rev. C* **17**, 1051 (1978).
- [13] D. Zubarev, V. Morozov, and G. Röpke, *Statistical Mechanics of Non-equilibrium Processes II* (Wiley, 1997).
- [14] B. Abelev *et al.* (ALICE), Pion, Kaon, and Proton Production in Central Pb–Pb Collisions at $\sqrt{s_{NN}} = 2.76$ TeV, *Phys. Rev. Lett.* **109**, 252301 (2012), arXiv:1208.1974 [hep-ex].
- [15] P. Braun-Munzinger and B. Dönigus, Loosely-bound objects produced in nuclear collisions at the LHC, *Nucl. Phys. A* **987**, 144 (2019), arXiv:1809.04681 [nucl-ex].
- [16] S. Acharya *et al.* (ALICE), Multiplicity dependence of π , K , and p production in pp collisions at $\sqrt{s} = 13$ TeV, *Eur. Phys. J. C* **80**, 693 (2020), arXiv:2003.02394 [nucl-ex].
- [17] D. Blaschke, G. Röpke, D. N. Voskresensky, and V. G. Morozov, Nonequilibrium pion distribution within the Zubarev approach, *Particles* **3**, 380 (2020), arXiv:2004.05401 [hep-ph].
- [18] J. Weil, V. Steinberg, J. Staudenmaier, L. G. Pang, D. Oliinychenko, J. Mohs, M. Kretz, T. Kehrenberg, A. Goldschmidt, B. Bäuchle, J. Auvinen, M. Attems, and H. Petersen, Particle production and equilibrium properties within a new hadron transport approach for heavy-ion collisions, *Phys. Rev. C* **94**, 054905 (2016).
- [19] J. Auvinen, K. J. Eskola, P. Huovinen, H. Niemi, R. Paatelainen, and P. Petreczky, Temperature dependence of η/s of strongly interacting matter: Effects of the equation of state and the parametric form of $(\eta/s)(t)$, *Phys. Rev. C* **102**, 044911 (2020).
- [20] H. Jeffreys, *The theory of probability*, 3rd ed., Oxford Classic Texts in the Physical Sciences (Oxford University Press, London, England, 1998).
- [21] D. Blaschke, M. Cierniak, O. Ivanytskyi, and G. Röpke, Thermodynamics of quark matter with multi-quark clusters in an effective Beth-Uhlenbeck type approach, *Eur. Phys. J. A* **60**, 14 (2024), arXiv:2308.07950 [nucl-th].